A Bayesian astrochronology for the Cambrian first occurrence of trilobites in West Gondwana (Morocco)

Matthias Sinnesael, Andrew R Millard, Martin R Smith

A Bayesian astrochronology for the Cambrian first occurrence of trilobites in West Gondwana (Morocco)

Matthias Sinnesael[1,2,3], Andrew R. Millard[4], Martin R. Smith[1]

[1]Department of Earth Sciences, Durham University, Durham, UK

[2]IMCCE, CNRS, Observatoire de Paris, PSL University, Sorbonne Université, Paris, France

[3]Department of Geology, School of Natural Sciences, Trinity College Dublin, Ireland

[4]Department of Archaeology, Durham University, Durham, UK

ABSTRACT

The first occurrence of trilobites ~520 million years ago is an iconic feature of the Cambrian Explosion. Developing a robust evolutionary view on early Cambrian life is generally hindered by large uncertainties in the ages of fossil finds, and their global stratigraphic correlation. Here, we develop an astrochronological interpretation for the Tiout section in Morocco that features some of the oldest trilobite fossils. Our novel approach to incorporating individual astronomical cycle durations in an integrated radio-isotopic and astrochronological Bayesian age-depth model results in an age estimate of 519.62 Ma (519.70–519.54 Ma 95% highest posterior distribution) for the first occurrence of trilobites in West Gondwana. This level of precise age estimation is exceptional for biological events in deep time and demonstrates the power of our novel approach.

INTRODUCTION

Lower Cambrian (~540–520 million years ago, Ma) strata are marked by a prominent increase in abundance and diversity in the fossil record. Whether this increase reflects a fast evolutionary event, also known as the 'Cambrian Explosion' (Gould, 1989), or a more gradual mode of evolution (Wood et al., 2019) is an open question. The main challenges in resolving this question are large uncertainties in the stratigraphic framework and a lack of direct radioisotopic age control of fossil finds (Bowyer et al., 2022). Given the limitations of classical stratigraphic tools like biostratigraphy and magnetostratigraphy for lower Cambrian stratigraphy, carbon isotope ratio chemostratigraphy ($\delta^{13}C$) has become the main tool for global correlations (Tucker, 1986; Magaritz et al., 1991; Bowyer et al., 2022).

An iconic feature of the early Cambrian evolutionary transition is the first occurrence (FO) of trilobites. Some of the oldest trilobite fossils can be found in West Gondwana, corresponding to present-day southern Morocco (Landing et al., 2021). These Moroccan sections are also crucial for lower Cambrian stratigraphy due to extensive $\delta^{13}C$ chemostratigraphic and geochronological studies (Tucker, 1986; Compston et al., 1992; Maloof et al., 2005, 2010; Hay et al., 2019; Landing et al., 2021). While radio-isotope geochronology provides anchored numerical age information for individual horizons, astrochronology – i.e. the estimation of time based on the identification of astronomical cycles in the sedimentary record – has the complementary advantage of providing floating but continuous duration estimates (Laskar, 2020). Combining absolute age estimates of discrete beds with this continuous record of the passage of time across strata can further constrain temporal frameworks and correlations. Existing Bayesian age-depth models only use total astrochronological duration estimates for specific stratigraphic intervals (Meyers et al., 2012; De Vleeschouwer and Parnell, 2014). In this study, we present a high-resolution astrochronological age model for the FO of trilobites in Morocco, in the well-studied Tiout section. In addition, we

suggest a novel way to improve both precision and accuracy of integrated age-depth models by explicitly using individual astronomical cycles in an astrochronological Bayesian age-depth model.

MATERIALS AND METHODS

The Tiout section consists of a series of clearly exposed lower Cambrian strata in a gorge south of Tiout village (30°23' N, 8°42' W; see Fig. 1 in Maloof et al. (2005) for a regional geological map). We digitized the quantified lithofacies and cyclothem identification reported in Monninger (1979). Chemical abrasion isotope-dilution thermal ionization mass spectrometry (CA-ID-TIMS) radio-isotopic dates and analytical uncertainty estimates are taken from Landing et al. (2021) as input for our age-depth models. All dates come from bentonite volcanic zircon samples, except for detrital zircons from a thin sandstone layer (Ti I-neg 8.5) near the base of the Tiout Member some 30 m above the level of first trilobite fragments that offer a maximal depositional age constraint (Landing et al., 2021).

We used the R package "astrochron" (Meyers, 2014; R core team, 2023) to conduct evolutive power spectral analysis (Thomson, 1982) and eTimeOpt analysis (Meyers, 2015, 2019). TimeOpt is a statistical optimization method that can simultaneously consider spectra distributions and amplitude modulation patterns to test for a precession-eccentricity origin in a signal. While TimeOpt uses a constant accumulation rate for the entire investigated section, eTimeOpt allows for changing accumulation rates using a moving window approach.

We built an integrated radio-isotopic plus astrochronological Bayesian age-depth model by expressing depth in units of sedimentary cycles, which the astrochronological interpretation infers are short eccentricity (SE) cycles (model A). This approach assumes constant accumulation rates

within a cycle, and the absence of substantial hiatuses. This depth scale was used for the positions of the radio-isotopic constraints; interpreted SE cycles; and the FO of trilobites. Following Landing et al. (2021), we used the lowest level of trilobite fragments, rather than the lowest level of identifiable trilobite species, to denote the local FO of trilobites. To build the age-depth model we used an Oxcal 4.4 (Ramsey, 2009) U-sequence assuming a fixed (but unknown) deposition rate per unit of depth model to relate these units to time. A prior distribution for the duration of the individual SE cycles with a mean of 96.5 k.y. (σ = 2 k.y.) was taken from Lantink et al. (2022), who investigated the time differences between successive maxima in full eccentricity solution curves, rather than considering only the duration of the SE cycle that has multiple components around ~100 k.y.. To evaluate our new model, we also constructed two reference Oxcal age-depth models that do not employ astrochronological data – conceptually similar to Landing et al. (2021), who used the "modifiedBchron" package (Trayler et al., 2020). The first radio-isotopic age-depth model (model B) only considers ages from volcanic zircons whose ages represents the date of deposition (bentonites labelled as Ti566 – assumed to be equivalent with M236 from Maloof et al. (2010), Am0.0 and Am34.0 in **Fig. 2A**) using an Oxcal P-sequence model (Ramsey, 2008; Ramsey and Lee, 2013). The Oxcal P-sequence models sediment deposition as a series of discrete deposits of sediment, with the number of events per unit length of section following a Poisson distribution, and the parameter of the distribution to be inferred. Our second radio-isotopic age-depth model (model C) uses an additional date from detrital zircons (Ti I-neg 8.5) to contain the maximal depositional age of its depth. The digitized lithofacies, R spectral analysis script and Oxcal age-depth models are available in the **Supplemental Material**.

RESULTS AND DISCUSSION

Cyclostratigraphic Analysis

The lower Cambrian strata of Tiout are characterized by regular alternations of darker limestones with lighter-colored marlstones that are clearly developed in the Lie de Vin and Igoudine formations (Monninger, 1979; **Fig. 1A**). Individual beds and cycles can be traced for many kilometres, whereas the lithological expression of cycles can vary slightly according to the stratigraphic and regional position (Monninger, 1979; **Fig. 1**). Monninger (1979) constructed a detailed lithofacies log that he also converted into a discretized numerical log, with its two end-members being shaly siltstones (low values) and dark, often biohermal, limestones (high values) (**Fig. 2B**). He also recognized several orders of bundled cyclicity with: a basic ~5-m 'rhythm'; ~25-m 'cyclothems' consisting of several rhythms; ~100-m 'supercycles'; and a 'long term trend' (**Fig. 1B**). Spectral analysis of the digitized lithofacies confirms the presence of the 'rhythms' (4.5–6.0 m) and 'cyclothems' (20–30 m) (**Fig. 2C**). The evolutive power spectral analysis suggests that these cycles are relatively constant in thickness and are especially clearly developed in the middle and upper Lie de Vin Formation (Fm.) (**Fig. 2C**). An eccentricity–precession origin of the cyclothems and rhythms is suggested by the ratio between the thicknesses of the different cycles and the clear amplitude modulation pattern expressed as the bundled alternations of intervals with clearer and darker limestones beds with lighter marlstones alternating with intervals with less distinguishable limestone-marlstone couplets (**Fig. 1**). The rhythm/cyclothem thickness ~1:5 to 1:6 ratio is also close to the early Cambrian short to long obliquity duration ratio (Laskar, 2020; Farhat et al., 2022).

These hypotheses can be independently tested using the exceptional availability of multiple volcanic zircon CA-ID-TIMS U-Pb ages. These ages occur throughout the studied interval, and bracket it stratigraphically (**Fig. 2A**). When dividing the time difference between the bentonite

ages by the number of cyclothems *sensu* Monninger (1979) in between the bentonites, each cyclothem has an average duration of ~100 k.y. (84–116 k.y. considering both minimal and maximal U-Pb duration and cycle number estimates), consistent with a SE interpretation (**Fig. 2A**). This is also an argument for the relative stratigraphic completeness of the section on at least the ~100 k.y. time scale. Moreover, the long-term U-Pb derived average accumulation rates are in the order of ~260 m m.y.$^{-1}$ (**Fig. 3**). This is close to the optimal solution obtained by eTimeOpt analysis (~250 m m.y.$^{-1}$; **see the Supplemental Material**), and suggests that the ~5 m 'rhythms', ~25 m 'cyclothems' and ~100 m 'supercycles' correspond with the expected Cambrian periodicities of ~19 k.y. climatic precession, ~100 k.y. SE and 405 k.y. long eccentricity (Laskar, 2020; Farhat et al., 2022). The long eccentricity periodicity is less prominent, both statistically and visually. This might be explained by non-astronomically driven changes in the sedimentary environment (e.g. tectonic evolution or sea-level changes) that occurred on similar timescales.

We have provided the first demonstration of an astronomical origin for the lithological cycles in the Lie de Vin and Igoudine formations, in contrast to previous suggestions of an autocyclic origin (Monniger, 1979; Maloof et al., 2005). We suggest that changes in detrital terrigenous input (Monniger, 1979) reflect astronomically forced changes in climate by precession forcing of the monsoonal circulation, in turn controlling precipitation patterns, and thus the transport of siliciclastic sediment (Wang et al., 2014; Sinnesael et al., 2021). Because strong precession signals are most evident in low-latitude monsoon-dominated climatic regimes, the prominent expression of such cyclicity in Morocco hints that Gondwana occupied a low rather than high paleolatitude, potentially informing the contested configuration of Cambrian paleocontinents (Wong Hearing et al., 2021; Keppie et al., 2023).

A Bayesian Astrochronology

Having established that the section is complete on the 100 k.y. scale, and that the 'cyclothems' correspond to SE cycles, we included the cyclothems as additional constraints in a Bayesian age-depth model for the Tiout section, resulting in a median age estimate for the FO of trilobites of 519.62 Ma (519.70–519.54 Ma 95% highest posterior distribution, or HPD, model A) (**Fig. 3**). The posterior distribution for the cyclothem duration in model A resulted in a median duration of 96.3 k.y. (92.5-99.9 k.y. 95% HPD), further supporting our SE interpretation. The median age estimates of both our radio-isotopic only models, with (519.75 Ma, 519.98-519.47 Ma 95% HPD, model C) and without (519.76 Ma, 520.10-519.41 Ma 95% HPD, model B) detrital zircon constraints, are close to each other, with a slightly broader HPD interval for model B. In our model the detrital age constraint serves as a simple maximum age for that depth. Landing et al. (2021) created a probability density function applying a uniform probability between the detrital age constraint and that of the next overlying volcanic zircon age – reasoning that the depositional age cannot be younger than the age of the overlying volcanic ash. Their approach resulted in an older trilobite FO age estimate of 519.95 Ma (520.38-519.55 Ma 95% highest density interval) overlapping with our preferred estimate of 519.62 Ma (519.70–519.54 Ma 95% HPD), but being about 320 k.y. older and ~5 times less precise. Our new younger astrochronological age estimate is the result of the additional cycle information incorporated, showing that accumulation rates were lower in the Lie De Vin Fm. and increased towards the Igoudine Formation (**Fig. 3)**.

Precise and accurate age determinations within deep-time biological transitions like the Cambrian Explosion are needed worldwide to resolve their detailed evolutionary dynamics. Zhang et al. (2022) constrained the FO of trilobite fossils in South China using a floating astrochronology based on the 405 k.y. eccentricity cycle that was anchored on a correlated SHRIMP U-Pb age

(Compston et al., 2008) whose low precision of 1.90 m.y. dominates the final uncertainty estimate of 1.91 m.y.. The FO of trilobite fossils in Avalonia is best constrained by a dated ash bed around the local level of trilobite FO in Wales (UK) with an age of 519.30 ± 0.77 Ma (including tracer calibration and ^{238}U decay constant errors; Harvey et al., 2011). Other sections worldwide lack any form of direct age control and their stratigraphic position of the local FO of trilobite fossils is usually based on $\delta^{13}C$ correlations. For example, the oldest trilobite fossil remains are thought to be documented in Siberia, occurring below the peak of the IV $\delta^{13}C$ excursion (Varlamov et al., 2008; Bowyer et al., 2023), while they occurred above the IV $\delta^{13}C$ excursion in the Moroccan sections (Tucker, 1986). Unfortunately, the $\delta^{13}C$ profile of the Tiout section only features low-resolution $\delta^{13}C$ data, in contrast to other Cambrian sections in southern Morocco (Maloof et al., 2005), and we therefore only present a conservative age estimate for the IV $\delta^{13}C$ peak as discussed in the **Supplemental Material**. While improving age estimates for biostratigraphic horizons it stays crucial to keep in mind geographic, environmental, and taphonomic controls on fossil occurrences too (Cramer et al., 2015; Landing et al., 2021).

CONCLUSIONS

We demonstrated an astronomical origin for the enigmatic lithological alternations of the lower Cambrian section of Tiout, Morocco and showed how explicitly using individual astronomical cycles in a Bayesian age-depth model can improve both the precision and accuracy of the FO of trilobite fossils in West Gondwana (519.62 Ma, 519.70–519.54 Ma 95% HPD). Our work further demonstrates the potential for the use of astrochronology, preferably with multiple high-quality radio-isotopic constraints from the same section, to better constrain time scales and major changes in the evolution of life – especially in deep-time intervals where many other

classical stratigraphic tools like biostratigraphy or magnetostratigraphy have limited utility. Similar work in time-equivalent sections worldwide may yield the equally high-quality age estimates of chemostratigraphic events, FO of trilobite fossils, and other Fortunian taxa that currently continue to suffer from exceedingly poor age control required to resolve their precise evolutionary dynamics.

ACKNOWLEDGMENTS

We thank M. Schmitz, G. Geyer and E. Landing for initial discussion on the Tiout section, and C. Bronk Ramsey for advice on OxCal coding. This contribution is supported by Leverhulme Trust Research Project Grant 2019-223 to M.R.S., and M.S. is funded by the ERC under the EU's Horizon 2020 research and innovation programme (advanced grant no. AstroGeo-885250). This work contributes to IGCP projects 652 and 735. For the purpose of open access, the author has applied a Creative Commons Attribution (CC BY) license to any Author Accepted Manuscript version arising from this submission.

REFERENCES CITED

Bowyer, F.T., Zhuravlev, A.Y., Wood, R., Shields, G.A., Curtis, A., Poulton, S.W., Condon, D.J., Yang, C., and Zhu, M., 2022, Calibrating the temporal and spatial dynamics of the Ediacaran-Cambrian radiation of animals: Earth-Science Reviews, 225, p. 103913, https://doi.org/10.1016/j.earscirev.2021.103913.

Bowyer, F.T., Zhuravlev, A.Y., Wood, R., Zhao, F., Sukhov, S.S., Alexander, R.D., Poulton, S.W., and Zhu, M., 2023, Implications of an integrated late Ediacaran to early Cambrian

stratigraphy of the Siberian Platform, Russia. GSA Bulletin, v. 135, p. 2428-2450, https://doi.org/10.1130/B36534.1.

Bronk Ramsey, C., 2008, Deposition models for chronological records: Quaternary Science Reviews, v. 27, p. 42–60, https://doi.org/10.1016/j.quascirev.2007.01.019.

Bronk Ramsey, C., 2009, Bayesian Analysis of Radiocarbon Dates: Radiocarbon, v. 51, p. 337-360, https://doi.org/10.1017/S0033822200033865.

Bronk Ramsey, C., and Lee, S., 2013, Recent and Planned Developments of the Program OxCal: Radiocarbon, v. 55, p. 720-730, https://doi.org/10.1017/S0033822200057878.

Compston, W., Williams, J.L., Kirschvink, J.L., Zhang, Z.W., and Ma, G., 1992, Zircon U-Pb ages for the Early Cambrian time scale: Journal of the Geological Society of London, v. 127, p. 319–32, https://doi.org/10.1144/gsjgs.149.2.0171.

Compston, W., Zhang, Z., Cooper, J.A., Ma, G., and Jenkins, R.J.F., 2008, Further SHRIMP geochronology on the early Cambrian of South China: American Journal of Science, v. 308, p. 399–420, https://doi.org/10.2475/04.2008.01.

Cramer, B.D., Vandenbroucke, T.R.A.V., and Ludvigson, G.A., 2015, High-Resolution Event Stratigraphy (HiRES) and the quantification of stratigraphic uncertainty: Silurian examples of the quest for precision in stratigraphy: Earth-Science Reviews, v. 141, p. 136-153, https://doi.org/10.1016/j.earscirev.2014.11.011.

De Vleeschouwer, D., and Parnell, A.C., 2014, Reducing time-scale uncertainty for the Devonian by integrating astrochronology and Bayesian statistics: Geology, v. 42, p. 491–494, https://doi.org/10.1130/G35618.1.

Farhat, M., Auclair-Desrotour, P., Boué, G., and Laskar, J., 2022, The resonant tidal evolution of the Earth-Moon distance: Astronomy & Astronphysics, v. 665, p. L1, https://doi.org/10.1051/0004-6361/202243445.

Gould, S.J., 1989, Wonderful Life: The Burgess Shale and the nature of history: New York, W.W. Norton, 347 p.

Harvey, T.H.P., Williams, M., Condon, D.J., Wilby, P.R., Siveter, D.J., Rushton, A.W.A., Leng, M.J., and Gabbott, S.E., 2011, A refined chronology for the Cambrian succession of southern Britain: Journal of the Geological Society, London, v. 168, p. 705–716, https://doi.org/10.1144/0016-76492010-031.

Hay, C.C., Creveling, J.R., Hagen, C.J., Maloof, A.C., and Huybers, P., 2019, A library of early Cambrian chemostratigraphic correlations from a reproducible algorithm: Geology, v. 47, p. 457-460, https://doi.org/10.1130/G46019.1.

Keppie, D.F., Keppie, J.D., and Landing, E., 2023, A tectonic solution for the Early Cambrian palaeogeographic enigma: Geological Society, London, Special Publications, v. 542, https://doi.org/10.1144/SP542-2022-35.

Landing, E., Schmitz, M.D., Geyer, G., Trayler, R.B., and Bowring, S.A., 2021, Precise early Cambrian U–Pb zircon dates bracket the oldest trilobites and archaeocyaths in Moroccan West Gondwana: Geological Magazine, v. 158, p. 219-238, https://doi.org/10.1017/S0016756820000369.

Lantink, M.L., Davies, J.H.F.L., Ovtcharova, M., and Hilgen, F.J., 2022, Milankovitch cycles in banded iron formations constrain the Earth–Moon system 2.46 billion years ago. PNAS, v. 119, p. e2117146119, https://doi.org/10.1073/pnas.2117146119.

Laskar, J., 2020, Chapter 4 – Astrochronology, *In* Gradstein, F.M., Ogg, J.O., Schmitz, M.D., and Ogg, G.M., eds., Geologic Time Scale 2020, Amsterdam, Elsevier, p. 139-158, https://doi.org/10.1016/B978-0-12-824360-2.00004-8.

Magaritz, M., Kirschvink, J.L., Latham, A.J., Zhuravlev, A.Y., and Razanov, A.Y., 1991, Precambrian/Cambrian boundary problem: Carbon isotope correlations for Vendian and Tommotian time between Siberia and Morocco: Geology, v. 19, p. 847-850, https://doi.org/10.1130/0091-7613(1991)019<0847:PCBPCI>2.3.CO;2.

Maloof, A.C., Schrag, D.P., Crowley, J.L., and Bowring, S.A., 2005, An expanded record of Early Cambrian carbon cycling from the Anti-Atlas Margin, Morocco: Canadian Journal of Earth Sciences, v. 42, p. 2195–2216, https://doi.org/10.1139/e05-062.

Maloof, A.C., Ramezani, J., Bowring, S.A., Fike, D.A., Porter, S.M., and Mazouad, M., 2010, Constraints on early Cambrian carbon cycling from the duration of the Nemakit-Daldynian–Tommotian boundary $\delta^{13}C$ shift, Morocco: Geology, v. 38, p. 623–626, https://doi.org/10.1130/G30726.1.

Meyers, S.R., Siewert, S.E., Singer, B.S., Sageman, B.B., Condon, D.J., Obradovich, J.D., Jicha, B.R., and Sawyer, D.A., 2012, Intercalibration of radioisotopic and astrochronologic time scales for the Cenomanian-Turonian boundary interval, Western Interior Basin, USA: Geology, v. 40, p. 7-10, https://doi.org/10.1130/G32261.1.

Meyers, S.R., 2014, Astrochron: An R Package for Astrochronology: http://cran.r-project.org/package=astrochron (accessed April 2023).

Meyers, S.R., 2015, The evaluation of eccentricity-related amplitude modulation and bundling in paleoclimate data: An inverse approach for astrochronologic testing and time scale

optimization: Paleoceanography, v. 30, p. 1625–1640, https://doi.org/10.1002/2015PA002850.

Meyers, S.R., 2019, Cyclostratigraphy and the problem of astrochronologic testing: Earth-Science Reviews, v. 190, p. 190–223, https://doi.org/10.1016/j.earscirev.2018.11.015.

Monninger, W., 1979, The section of Tiout (Precambrian/Cambrian boundary beds, Anti-Atlas, Morocco): an environmental model [Ph.D. thesis]: Arbeiten aus dem Paläontologischen Institut Würzburg 1, 289 p.

R Core Team, 2023, R: A Language and Environment for Statistical Computing: Vienna, R Foundation for Statistical Computing, http://www.r-project.org.

Sinnesael, M., McLaughlin, P.I., Desrochers, A., Mauviel, A., De Weirdt, J., Claeys, P., and Vandenbroucke, T.R.A, 2021, Precession-driven climate cycles and time scale prior to the Hirnantian glacial maximum: Geology, v. 49, p. 1295-1300, https://doi.org/10.1130/G49083.1.

Thomson, D.J., 1982, Spectrum estimation and harmonic analysis: Proceedings of the IEEE, v. 70, p. 1055–1096, https://doi .org/10.1109/PROC.1982.12433.

Trayler, R.B., Schmitz, M.D., Cuitiño, J.I., Kohn, M.J., Bargo, M.S., Kay, R.F., Strömberg, C.A.E., and Vizcaíno, S.F., 2020, An improved approach to age-modeling in deep time: Implications for the Santa Cruz Formation, Argentina: GSA Bulletin, v. 132, p. 233-244, https://doi.org/10.1130/B35203.1.

Tucker, M.E., 1986, Carbon isotope excursions in Precambrian/Cambrian boundary beds: Nature, v. 319, p. 48-50, https://doi.org/10.1038/319048a0.

Varlamov, A.I., Rozanov, A.Yu, Khomentovsky, V.V., Shabanov, Yu.Ya, Abaimova, G.P., Demidenko, Yu.E, Karlova, G.A., Korovnikov, I.V., Luchinina, V.A., Malakhovskaya,

Ya.E., Parkhaev, P.Yu, Pegel, T.V., Skorlotova, N.A., Sundukov, V.M., Sukhov, S.S., Fedorov, A.B., Kipriyanova, L.D., 2008, The Cambrian system of the Siberian Platform. Part 1: The Aldan–Lena Region. Field Conference of the Cambrian Stage Subdivision Working Group, Yukatia, Russia, July 20–August 1, 2008. PIN RAS, Moscow, Novosibirsk (300 pp.).

Wang, P.X., Wang, B., Cheng, H., Fasullo, J., Guo, Z.T., Kiefer, T., and Liu, Z.Y., 2014, The global monsoon across timescales: Coherent variability of regional monsoons: Climate of the Past, v. 10, p. 2007–2052, https://doi .org/10.5194/cp-10-2007-2014.

Wong Hearing, T.W., Pohl, A., Williams, M., Donnadieu, Y., Harvey, T.H.P., Scotese, C.R., Sepulchre, P., Franc, A., and Vandenbroucke, T.R.A., 2021, Quantitative comparison of geological data and model simulations constrains early Cambrian geography and climate: Nature Communications, v. 12, p. 3868, https://doi.org/10.1038/s41467-021-24141-5.

Wood, R., Liu, A.G., Bowyer, F., Wilby, P.R., Dunn, F.S., Kenchington, C.G., Hoyal Cuthill, J.F., Mitchell, E.G., and Penny, A., 2019, Integrated records of environmental change and evolution challenge the Cambrian Explosion: Nature Ecology & Evolution, v. 3, p. 528-538, https://doi.org/10.1038/s41559-019-0821-6.

Zhang, T., Lia, Y., Fan, T., Da Silva A.-C., Shi, J., Gao, Q., Kuang, M., Liu, W., Gao, Z., and Li, M., 2022, Orbitally-paced climate change in the early Cambrian and its implications for the history of the Solar System: Earth and Planetary Science Letters, v. 583, p. 117420, https://doi.org/10.1016/j.epsl.2022.117420.

FIGURE CAPTIONS

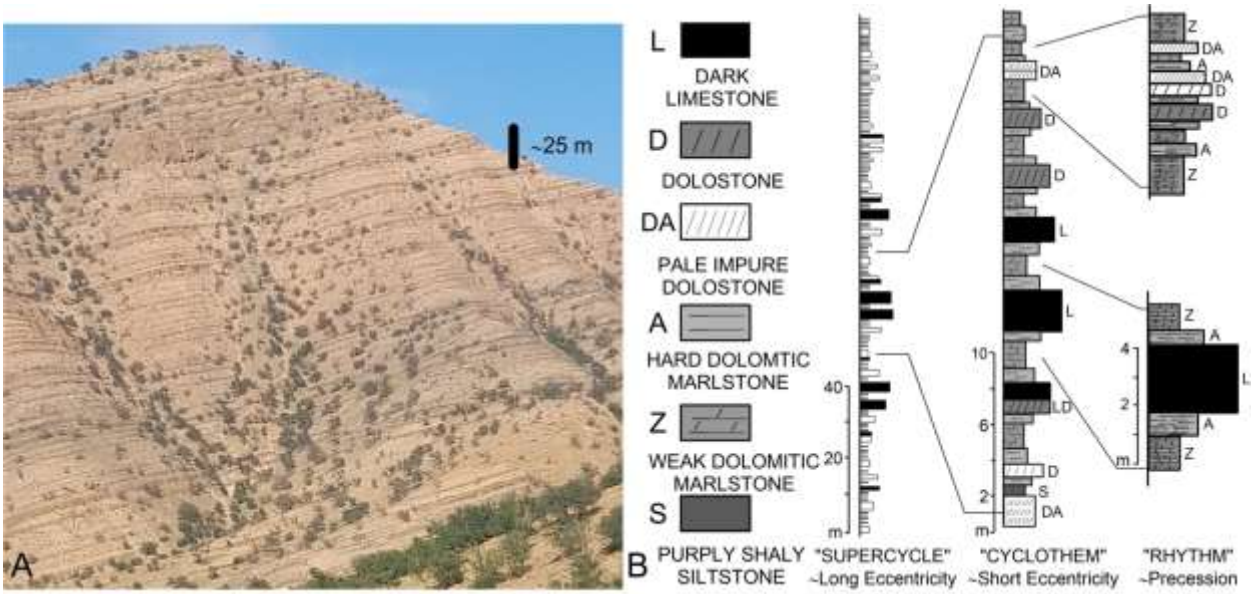

Figure 1: (A) Illustrative photograph of characteristic bundles of alternations between dark limestones and lighter marlstones in the Lie De Vin Formation ©Kilian Eichenseer. (B) Schematic representation of the different lithologies and various orders of lithological cyclicity (from Monninger, 1979). The thickness ratios and bundling patterns suggest an eccentricity-precession signature of the cyclothems and rhythms, respectively.

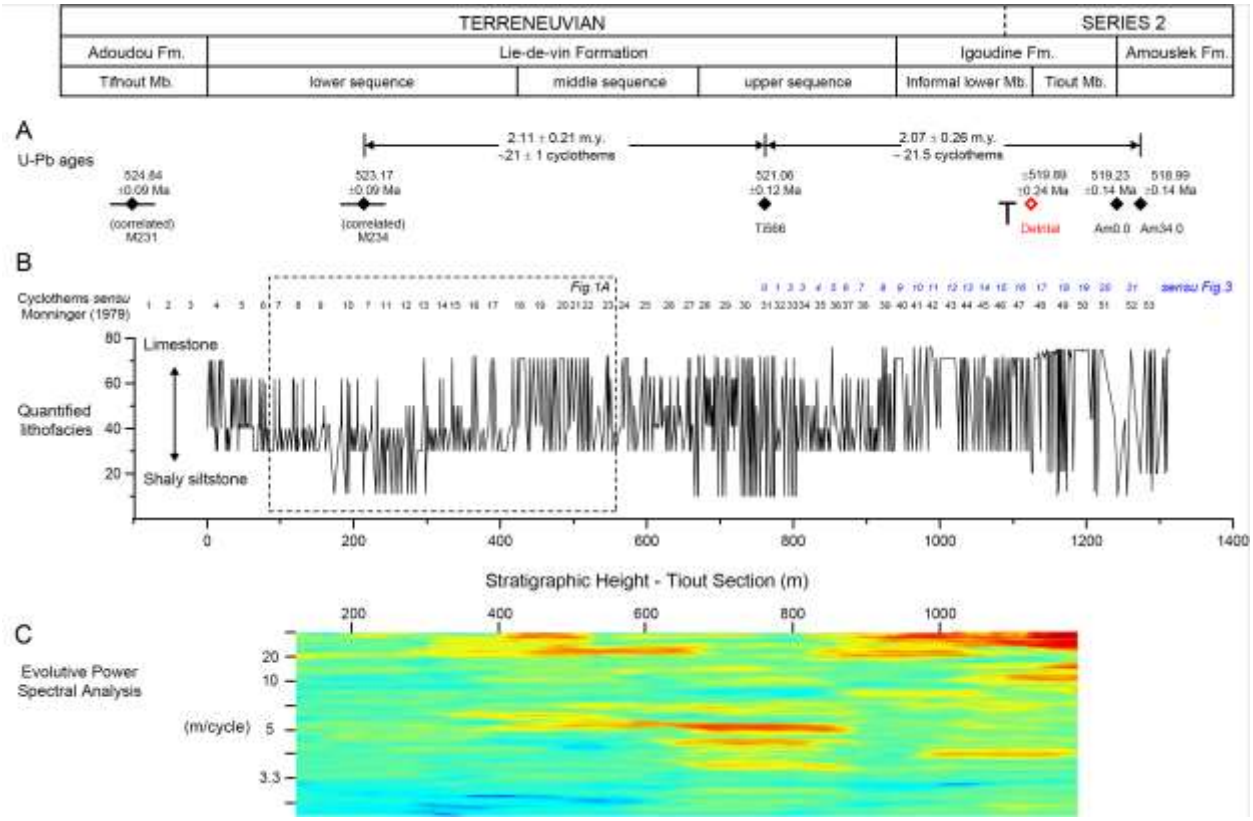

Figure 2: Stratigraphic overview of radio-isotopic age constraints and lithofacies of the Tiout section. (A) U-Pb radio-isotopic age constraints, following Maloof et al. (2010) for stratigraphically correlated bentonite samples M231 and M234, and Landing et al. (2021) for bentonites Ti566, Detrital, Am0.0 and Am34.0. 'T' indicates the position of the first trilobite fossil remains. (B) Quantified lithofacies and positions of cyclothems according to Monninger (1979). (C) Evolutive power spectral analysis of the lithofacies shown in Fig. 2B., with no results for the lowest and highest parts of the log because of the moving window approach (i.e. half the window size of 250 m).

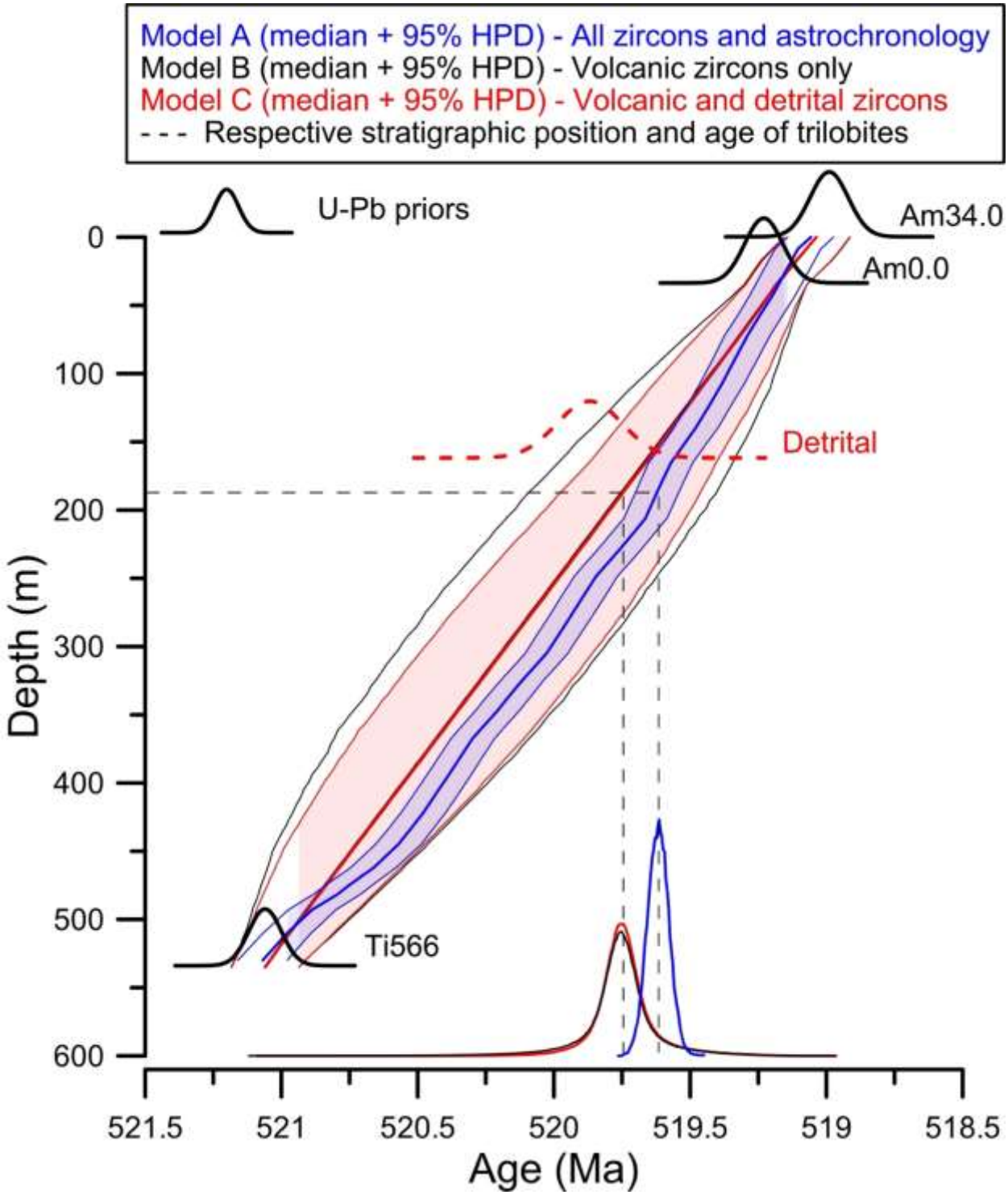

330

331 Figure 3: Our three OxCal Bayesian age-depth models for the Tiout section. The integration of
332 astrochronological information with the available U-Pb constraints (model A) makes the age
333 estimate for the first occurrence of trilobites in southern Morocco more precise and a few hundred

thousand years younger compared to estimates solely based on U-Pb constraints coming from volcanic zircons only (model B) and both volcanic and detrital zircons (model C). The depth scale for model A is calculated in function of number of cycles and rescaled to the depth-m-scale for plotting.

[1]Supplemental Material. *[Lithofacies log from Monniger 1979, time-series analyses script in R and Oxcal age-depth model files]* Please visit https://doi.org/10.1130/XXXX to access the supplemental material, and contact editing@geosociety.org with any questions.